

## NUMERICAL INVESTIGATION ON THE FRICTION WEDGE DAMPER DYNAMICS - A COMPARATIVE STUDY

**Henrique Brenner de Araújo, henriqueba@gmail.com**

Faculdade de Engenharia Mecânica, Universidade Estadual de Campinas  
Rua Mendeleev, 200 – Cidade Universitária, Campinas – SP, Brasil

**Leonardo Bartalini Baruffaldi, leobart@fem.unicamp.br**

Faculdade de Engenharia Mecânica, Universidade Estadual de Campinas

**Auteliano Antunes dos Santos Jr., aute@fem.unicamp.br**

Faculdade de Engenharia Mecânica, Universidade Estadual de Campinas

**Abstract.** Friction wedges are damping elements commonly used within the secondary suspension of freight railway cars, dissipating the vibrational energy through dry friction. It is known that this type of friction force introduces singularities to the behavior of the system. Hence, the equations of motion become non-linear, giving rise to stick-slip phenomena near certain frequencies which results in non-smooth differential equations. Several studies showed that linear or quasi-linear models of such systems do not describe it properly. This paper presents a multibody model of the bogie's secondary suspension and its simulation results for three different friction laws and then compares these results with previously published experimental data.

**Keywords:** three-piece freight car truck, friction wedge damper, multibody dynamics, stick-slip

### 1. INTRODUCTION

The three-piece-truck or bogie has been the standard railway freight wagon basis for more than 150 years (Hawthorne, 1996). It is a simple and trustfully mechanical assembly that supports the wagon weight and acts as an interfacial element between the rail and the load. It is composed of three main assemblies: the wheel sets (two per bogie), comprising the wheels and their axis, two side frames, structural members that directly support the wheels, and the bolster, a large traverse that holds the wagon itself. Usually the three-piece-truck suspension is studied in separated ways being the primary suspension the very stiff connection between the side-frame and axis, via bearings, and the secondary suspension the pack of springs and wedge dampers that connect the bolster to the side frame.

The friction wedges are the damping elements of the secondary suspension of three-piece freight truck. According to Hawthorne (1996), they have been in use since 1935 and the basic design hasn't changed much in the past seventy years. These devices are cast iron blocks with two angled surfaces that may slide with the other pieces of the bogie. There are two main types of friction wedges assemblies: with variable damping – when a spring forces the wedge against the friction surfaces – and with constant damping – if the wedge is housed directly in the bolster. Figure 1 gives a representation of these two types of suspension.

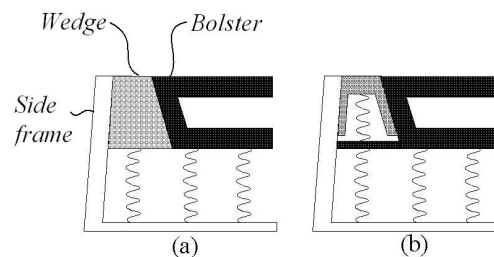


Figure 1. Variable (a) and constant (b) damping friction wedge configurations. The spring in the constant damping model acts only to keep contact pressure if the wedge gets loose due to surface wear.

The interest in mathematically modeling these dampers arose from the development of faster railways, which demand more reliable suspension systems to prevent wagon rollover, hunting and, ultimately, freight safety. However, due to the strong presence of dry friction, the equations of motion of even a simplified model of wedge damper are strongly non-linear. In the specific case of friction wedges, these equations are not prone to linearization around realistic operation conditions due to stick-slip dynamics, as was noticed by Gardner and Cusumano (1997). The phenomenon of stick-slip appears in all friction oscillators and occurs when the restitution forces (either spring-like or external) are not enough to overcome frictional resistance. Several authors addressed this subject (Feeny and Moon, 1993; Leine *et al.*,

1998; Hinrichs *et al.*, 1998).

Kaiser *et al.* (2002) presented a mechanical model for the vertical movements of the secondary suspension and studied its response to harmonic track input for several frequencies and amplitudes combinations with three different dry friction models. The numerical results showed that for small excitation frequencies (below resonance) the friction wedge causes strong stick-slip between the bolster and the side-frame. These results complain with those found by Hinrichs *et al.* (1996), who conducted an experimental and numerical research on the behavior of a simple mass-spring-damper oscillator in the presence of three different dry friction laws. Hinrichs also proposed a numerical friction model that takes into account the stochastic nature of frictional efforts.

Based on Kaiser's model, Chandiramani *et al.* (2006) made an experimental analysis of a three-piece truck's secondary suspension with a reduce scale model. Their results showed a stick-slip high frequency behavior that was not predicted by numerical models.

The present paper addresses this conflict between the experimental and numerical results by simulating a multibody system based on Chandiramani's prototype with an industry mainstream software (ADAMS/Solver). The equations of motion are generated directly on the program that allows for easy modification of simulation parameters. By comparing the results with sound experimental data, one can evaluate if the friction models proposed can represent real events.

## 2. FRICTION LAWS

Usually the friction characteristic is described by a function of the relative velocity  $v_r$  of the contacting surfaces, though experimental evidence shows that it may be affected by other state variables, particularly near the stick mode ( $v_r = 0$ ) (McMillan, 1997).

For this work, three different velocity-dependent models will be addressed: the Coulomb model, static-dynamic model and exponential model.

### 2.1. Coulomb friction

Coulomb's friction law is perhaps the most widely known formulation. This model supposes friction does not depend on the exact magnitude of the relative velocity, but only on its signal:

$$F_{a,I} = F_n \cdot \mu_d \text{sign}(v_r) \quad (1)$$

where  $F_{a,I}$  is the Coulomb friction force,  $F_n$  is the applied normal force and  $\mu_d$  is the dynamic coefficient of friction, which, in this case, has the same value as the static coefficient of friction. Figure 2(I) shows the plot of this law with respect to relative velocity.

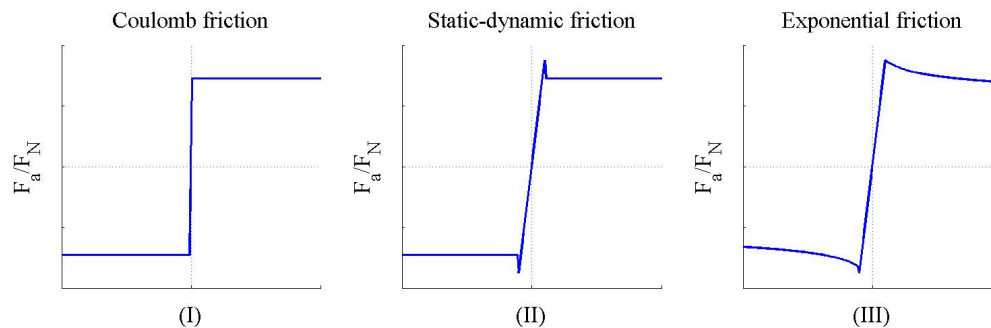


Figure 2. Comparison between friction laws.

### 2.2. Static-dynamic friction

The simple Coulomb model showed above does not consider that static friction (the force at very small relative velocities, when shear displacement is predominant) is slightly superior to dynamic. The static-dynamic friction model used attempts to improve the quality of the response when the relative velocity of the contacting surfaces approaches zero. Equation (2) gives the form of this law.

$$F_{a,II} = \begin{cases} F_n \cdot \mu_s \frac{v_r}{v_t} & , \text{ for } |v_r| \leq v_t \\ F_n \cdot \mu_d \text{sign}(v_r) & , \text{ for } |v_r| > v_t \end{cases} \quad (2)$$

where  $F_{a,II}$  is the static-dynamic friction force,  $\mu_s$  is the static coefficient of friction and  $v_t$  is a threshold velocity that was assumed as 1 mm/s, according to McMillan (1997). The profile of this law is depicted in Fig. 2(II).

### 2.3. Exponential model

The exponential model used in the present work is described by Eq. ( 3 ) and illustrated by the curve in Fig. 2(III).

$$F_{a,III} = \begin{cases} F_n \cdot \mu_s \frac{v_r}{v_t} & , \text{for } |v_r| \leq v_t \\ F_n \cdot \mu_d \text{sign}(v_r) \cdot v_r^{-0.1} & , \text{for } |v_r| > v_t \end{cases} \quad (3)$$

where the relative velocity exponent may be modified to adjust the model behavior. The main difference between this model and the static dynamic law is that here the friction decreases slightly with velocity.

## 3. PHYSICAL MODEL

The physical model used for simulations was chosen to be the same proposed by Chandiramani *et al.* (2006) to permit a reasonable evaluation of friction law effects on high frequencies and to allow for a comparison between the present work results and the experimental tests conducted by these authors. It is interesting to notice that this type of comparison between computational and empirical results for dry friction harmonically excited systems was already made by Hinrichs (1998) for a one degree of freedom mass-spring-damper oscillator over a conveyor belt and the results matched quite well. As commented, while theoretical models shows strong stick-slip below resonance, the prototype tested by Chandiramani presents a non-linear transition phase (from stick-slip to pure slip) near frequencies that are two to three times higher than the resonance peak.

While Kaiser *et al.* (2002) proposed the solution of the equations of motion with a piecewise integration algorithm, this work relies on a commercially available solver suited for stiff systems integration (GSTIFF, the standard ADAMS' solver). GSTIFF is a high performance solver that can handle non-smooth equations providing its parameters are correctly adjusted.

The characteristics of the model addressed are the same used on the machining of Chandiramani's prototype to seek its reproduction. Table 1 summarizes the physical parameter while Fig. 3 gives a graphical representation of one half of the three-piece truck's secondary suspension. The friction forces appear on the contact surfaces pair bolster/wedge and wedge/side frame, and the measured quantities were the relative velocity,  $dx/dt - dy/dt$ , and displacement,  $x - y$ , between the bolster and the side frame. It must be noticed that the physical parameters used by Chandiramani and reproduced here do not match for real railway suspensions; the angles of the wedge are, however, correct, and to a great extent they determine the way friction forces induces stick-slip on the system.

Table 1. Secondary suspension parameters

Parameter	Value
Wedge mass ( $M_w$ )	0.17 kg
Bolster mass ( $M_b$ )	0.70 kg
Side frame mass ( $M_{sf}$ )	0.46 kg
Stiffness of each wedge's spring ( $k_w$ )	2.55 N/mm
Stiffness of bolster's spring ( $k_b$ )	5.10 N/mm
Wedge angle ( $\alpha$ )	37.50 °
Side frame angle ( $\gamma$ )	4°
Dynamic friction coefficient ( $\mu_d$ )	0.29
Static friction coefficient ( $\mu_s$ )	0.32

## 4. MULTIBODY MODEL

To study the dynamical behavior of the friction wedge damper, a multibody model of half a three-piece truck was assembled on the mechanical simulation software MSC.ADAMS/View. The system consists of four bodies: the side-frame, which receives the efforts from the rail track; the bolster, an intermediate component between the wheel-set and the wagon itself; and two friction wedges, placed between the side-frame and the bolster. To constrain the movement to the  $xy$  plane, the interactions between these bodies were modeled as translational type joints. The movement was constrained to avoid the influence of  $z$ -directed friction forces, which are coupled to the vertical movement, as shown by Xia (2002) and to improve model comparative capabilities for Chandiramani model is also mainly unidimensional.

The friction forces were applied at the center of the contacting surfaces. The normal forces, necessary to get the fric-

tion efforts, were taken from the reactions of the translational joints normal to the contact plane. Care was taken so that the geometrical characteristics of the model would not allow for bolster lift-off.

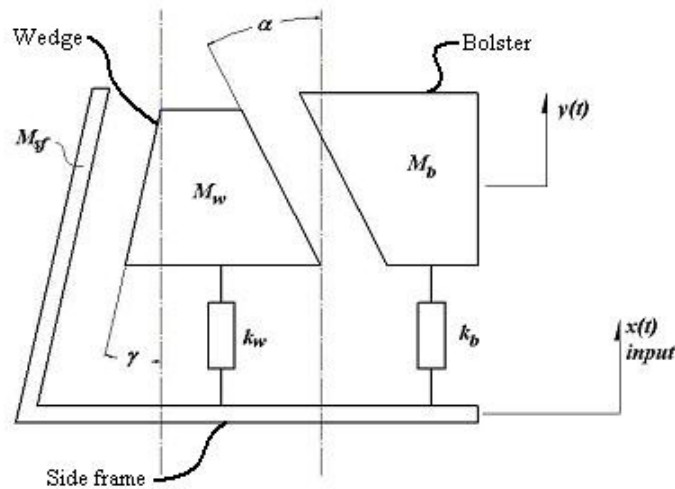


Figure 3. Physical model of 1/4 of three-piece-truck's secondary suspension.

Two elastic elements representing coil springs connect the bolster to the side frame and two more, the wedges and the side frame. The friction between the parts was modeled as a relative velocity dependent force acting tangentially to the contact plane.

Input was imposed at the side frame center of gravity as a vertical ( $y$ -directed) sinusoidal displacement in the form:

$$x(t) = a \cdot \sin(\beta \cdot \omega_n \cdot t) \quad (4)$$

where  $a$  is the input amplitude,  $t$  is elapsed time,  $\beta$  is a non-dimensional frequency factor and  $\omega_n$  is the bolster's natural frequency, which is given by:

$$\omega_n = \sqrt{\frac{k_b}{M_b}} = 85.35 \text{ rad/s} \quad (5)$$

## 5. ANALYSIS RESULTS

The model was simulated for input amplitudes varying from 0.005 mm to 4.750 mm and values of  $\beta$  ranging from 0.1 to 3.0 (equivalent to a frequency variation from 1.36 Hz to 40.76 Hz) with the three friction laws previously presented, resulting 1800 analysis cases. The frequency values were chosen to establish the connection between the analysis showed in Kaiser *et al.* (2002) and Chandiramani *et al.* (2006). The first presented analytical results for  $\beta$  varying from 0 to 1 and the second conducted experiments with  $\beta$  going from about 1.8 to 3.0.

All simulations started at the equilibrium position  $y_0 = -2.1941$  mm. The transient response of the analyses was left aside and only the steady state was considered. The total simulation time was set to 1.5 seconds but to the final analysis it was tucked accordingly so that two to three periods of the response were represented, aiming for clarity.

Figure 4 exhibits the amplitude ratio between output and input signals. From the diagram, it can be seen that the amplitude gain of the system does not suffer from different friction models and follows approximately the same tendency line. The resonance appears when the exciting frequency is about 80% of  $\omega_n$ , and for high frequencies the amplification factor goes to one.

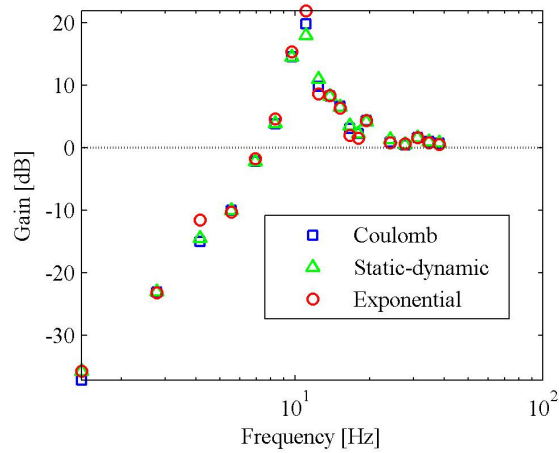


Figure 4. Amplitude ratios between input and output.

Figures 5 to 7 show the evolution of the system behavior with increasing values of  $\beta$ . The stick-slip appearance occurs until  $\beta = 0.4$  as Fig. 5 and Fig. 6 show. As general behavior it can be noticed that, for all tested frequencies and friction models, appreciable bolster/side frame displacement starts to show about  $a = 0.3$  mm. Below that input amplitude, the response is negligible.

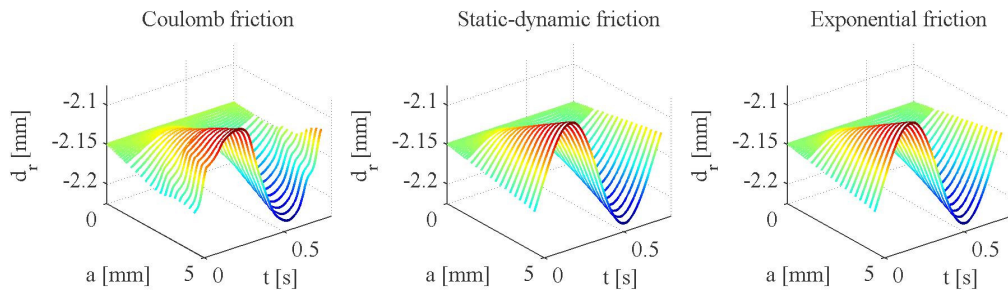


Figure 5. System response for  $\beta = 0.1$  (1.36 Hz). The  $d_r$  axis is the relative displacement.

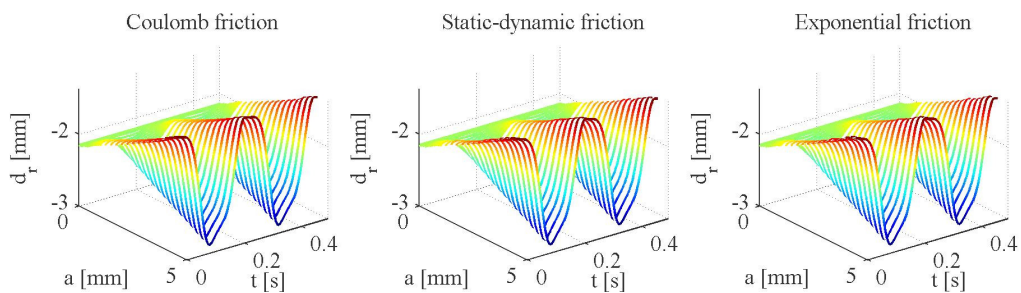


Figure 6. System response for  $\beta = 0.3$  (4.08 Hz).

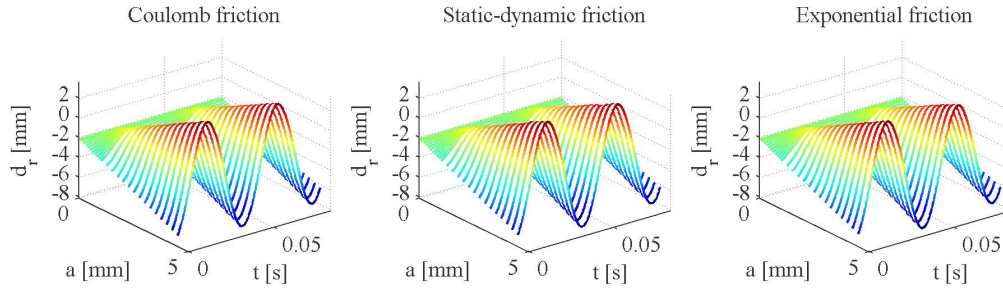


Figure 7. System response for  $\beta = 1.75$  (23.78 Hz).

The static-dynamic and the exponential laws resulted very similar behaviors. As it would be expected, near null velocity, i.e. in the region where the models try to deal with the discontinuity of friction, the static-dynamic and exponential laws follow slightly different time trajectories: the second approaches the Coulomb model while the other shows a less smoother behavior as a effect of the higher jump near transition velocity  $v_r$ . The influence of the friction model is even more evident if one analyses the period of the  $\beta = 0.1$  dataset, which is depicted in Fig. 5: while here both the static-dynamic and the exponential models do not exhibit stick-slip, the Coulomb law shows a distorted surface.

Figure 7 shows the system's general behavior for over-resonant frequencies: the response becomes almost sinusoidal and no relevant stick-slip phenomena were observed.

## 6. COMPARISON WITH EXPERIMENTAL CURVES

Though the results matched reasonably with other computational investigations (Kaiser *et al.*, 2002 and Hinrichs *et al.*, 1998), the proposed model and friction laws could not predict the high frequency stick-slip phenomena showed by Chandiramani *et al.* (2006).

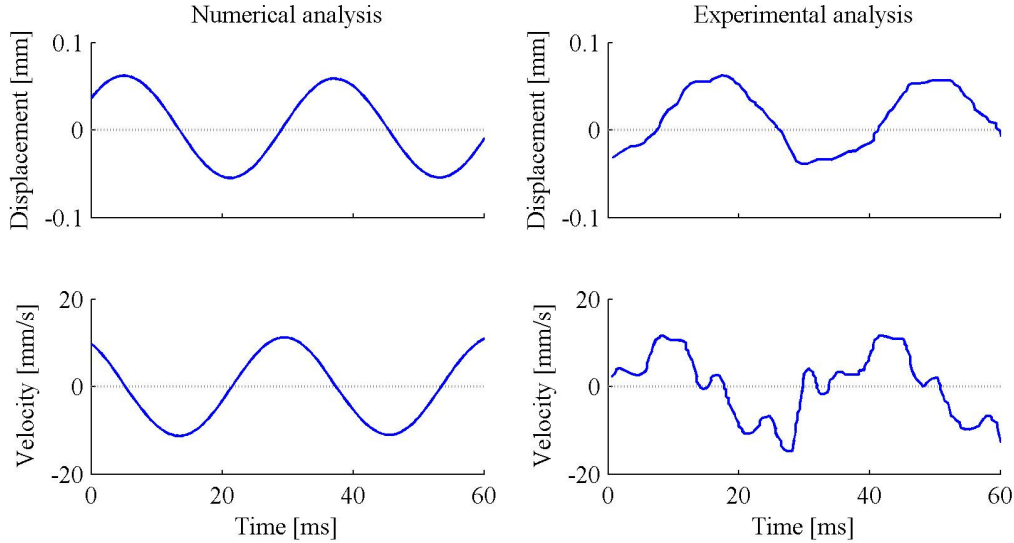


Figure 8. ADAMS (left) and Chandiramani's (right) experimental results for 30 Hz input compared.

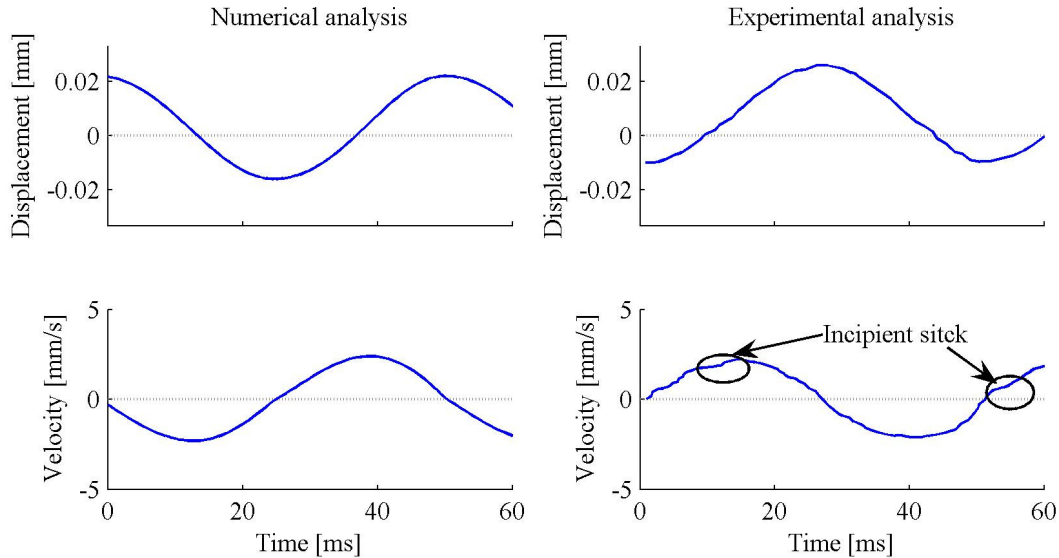


Figure 9. ADAMS (left) and Chandiramani's (right) experimental results for 20 Hz input compared.

Figure 8 shows the comparative curves for the 30 Hz responses with the Coulomb friction model. As observed previously, at over-resonant frequencies all friction laws tested presented similar behavior, so the following comments extend to both static-dynamic and exponential models. Because Chandiramani does not inform the input amplitude, the numerical result plotted is the one that most approaches the empirical peak-to-peak displacement response. In the case of Fig. 8, it was the 0.100 mm. The differences for this frequency are evident: while the numerical model ignores the presence of friction forces, responding like a usual harmonic oscillator, the experimental curve shows a highly distorted velocity profile.

Figure 9 shows a similar comparison between 20 Hz analyses. Again, as the experimental input amplitude was not given, the compared numerical result was the one that present the closest peak-to-peak response, in this case the 0.015 mm input. Here the differences between curves' shapes are not that evident, though careful examination of experimental velocity plot shows that the system starts to present stick tendency, as revealed by the arrows pointing small plateaus around 1/8 of the response period.

Another feature presented by Chandiramani *et al.* is the evolution of peak-to-peak response with respect to frequency. They noted that within the 20 Hz-40 Hz frequency range, this value increases initially slowly and, when frequency reaches about 35 Hz, it makes a jump towards a higher value. This also diverges from what was found by the present work: the numerical analysis showed that the output to input ratio increases until a resonance peak (around 11 Hz) and then decreases rapidly until it reaches and stabilizes at unit when input frequency is 20 Hz (Fig. 4).

## 7. CONCLUSION

A multi-body model of a simplified three-piece truck secondary suspension was assembled in ADAMS/View to investigate the dynamic behavior of the system. Three different friction models were applied to get a better insight of the effect of discontinuities on the harmonic response of the suspension.

The results of this computational model showed that stick-slip is a phenomenon that may occur at sub-resonant frequencies and appreciable input amplitude. At higher frequencies (noticeably at frequencies higher than the resonance), the presence of stick was not observed and the system responded as a non-frictional oscillator. These observations disagree with those presented in the experimental work by Chandiramani, which revealed the presence of sticking zones at frequencies 2 to 3 times higher than the natural frequency of the bolster assembly. The sources of this discrepancy may be divided into two branches: *numerical model errors* and *experimental model errors*.

Among the possible numerical model errors are the lack of two-dimensional friction – that may be interfering on Chandiramani's results at some extent – and incompleteness of friction models. Bad choices in integration methods are found to be an unlikely source of errors in this case for the qualitative form of the results agrees with other works published. The experimental model may also be defective, especially in two points: the small mass of the model may be sensing second order vibrations from sources that were disregarded on the numerical study presented, and the designed support that prevents the lateral movement of the suspension assembly may be permitting two-dimensional movement, affecting the results.

Usually, three-piece-trucks operate at low frequency ranges, making the under-resonant results especially important to the system dynamic. The comparison between the experimental and numerical results shows that at high frequencies

they do not agree at all, suggesting modeling and/or empirical errors. However, due to the absence of experimental data for small frequencies, a final conclusion on the real capacities of the multi-body model developed here is not possible, therefore new tests must be conducted before a sound wedge-damper model can be effectively applied on railcars suspension design.

## 8. REFERENCES

- Chandiramani, N. K., Srinivasan, K., and Nagendra, J., 2006, "Experimental Study of Stick-Slip Dynamics in a Friction Wedge Damper," *Journal of Sound and Vibration*, 291, pp. 1-18.
- Feeny, B. F., and Moon, F. C., 1993, "Bifurcation Sequences of a Coulomb Friction Oscillator," *Nonlinear Dynamics*, 4, pp. 25-37.
- Forbes, J. W., 2006, "Rail road car and truck therefor," US Patent 7004079.
- Gardner, J. F., Cusumano, J. P., 1997, "Dynamic Models of Friction Wedge Dampers," *Proc. of the 1997 ASME/IEEE Joint Railroad Conference*, Boston, Massachusetts, pp. 65-69.
- Hawthorne, V. T., 1996, "Recent Improvements to Three-Piece Trucks," *Proc. of the 1996 ASME/IEEE Joint Railroad Conference*, Oakbrook, Illinois, pp. 151-161.
- Hinrichs, N., Oestereich, M., and Popp, K., 1998, "On the Modelling of Friction Oscillators," *Journal of Sound and Vibration*, 216(3), pp. 435-459.a
- Kaiser, A. B., Cusumano, J. P., and Gardner, J. F., 2002, "Modeling and Dynamics of Friction Wedge Dampers in Railroad Freight Trucks," *Vehicle System Dynamics*, 38(1), pp. 55-82.
- Leine, R.I., van Campen, D. H., de Kraker, A., and van den Steen, L., 1998, "Stick-Slip Vibrations Induced by Alternate Friction Models," *Nonlinear Dynamics*, 16, pp. 41-54.
- McMillan, A. J., 1997, "A Non-Linear Friction Model for Self-Excited Vibrations," *Journal of Sound and Vibration*, 205(3), pp. 323-335.
- Xia, F., 2002, "Modelling of Wedge Dampers in the Presence of Two-Dimensional Dry Friction," *Vehicle System Dynamics Supplement*, 37, pp. 565-578.